

Measurement of the $^1\text{H}(\gamma, \pi^0)$ cross section near threshold. II. Pion angular distributions

J. C. Bergstrom, R. Igarashi, and J. M. Vogt

Saskatchewan Accelerator Laboratory, 107 North Road, University of Saskatchewan, Saskatoon, Saskatchewan, Canada S7N 5C6

(Received 4 October 1996)

This paper represents a continuation of our earlier report on the measurement of the reaction $^1\text{H}(\gamma, \pi^0)$ in the threshold region (144.7–169.3 MeV). More specifically, we present pion angular distributions reconstructed using information on the π^0 -decay photon energies not previously utilized. Analysis of these distributions reconfirms most of our previous conclusions. In particular, we confirm the rapid increase in the real part of the S -wave multipole, $\text{Re } E_{0+}$, at energies above the π^+ threshold. New results for the P -wave amplitude P_1 are presented. [S0556-2813(97)04504-4]

PACS number(s): 25.20.Lj, 13.60.Le

I. INTRODUCTION

In a previous Rapid Communication [1] we presented a brief summary of our measurements of the reaction $^1\text{H}(\gamma, \pi^0)$ within 25 MeV of threshold, using tagged photons and a large acceptance π^0 spectrometer (“Igloo”). Those measurements actually represent two separate experiments. The first experiment was devoted solely to the determination of the total cross section for the reaction. Here the π^0 spectrometer was configured for maximum π^0 acceptance (about 83% efficiency), but yielded virtually no useful information on the pion angular distributions. In the second experiment the π^0 spectrometer was reconfigured for maximum angular sensitivity (but at somewhat reduced efficiency) in order to measure the pion angular distributions. Through a combined analysis of both experiments the S -wave amplitude E_{0+} and certain combinations of the P -wave amplitudes were deduced as a function of energy. A reasonable model for the imaginary component $\text{Im } E_{0+}$ based on unitarity arguments permitted a separation of the real part $\text{Re } E_{0+}$ (see Fig. 4 in [1]). The rapid decrease in $\text{Re } E_{0+}$ observed between π^0 and π^+ thresholds (144.7 and 151.4 MeV, respectively) is characteristic of a unitarity cusp and has its genesis in the isospin splitting of the pion masses.

However, it is the region above π^+ threshold that is the main focus of the present paper, where $\text{Re } E_{0+}$ shows a fairly rapid recovery with increasing energy. We have argued in a recent note that just such a behavior can be expected from rather elementary phenomenological considerations [2]. These considerations suggest that the unitarity cusps in $\text{Re } E_{0+}$ and in the proton Compton amplitude $\text{Re } f_{EE}^+$ should be similar in shape. Certainly, the Compton amplitude exhibits a rapid change above the π^+ threshold as demonstrated in Ref. [3], not unlike the shape of $\text{Re } E_{0+}$.

At a more fundamental level, the recent chiral perturbation theory (CHPT) calculations of $\text{Re } E_{0+}$ by Bernard *et al.* [4] provide a reasonable accounting of the experimental amplitude between the π^0 and π^+ thresholds [1], but predict a much slower rate of increase above the π^+ threshold than observed. Whether the situation would change under a full one-loop calculation with isospin splitting is not presently known.

In this paper we will revisit this energy domain, but now

incorporate certain experimental information not previously utilized in [1], specifically improved knowledge of the π^0 -decay photon energies as provided by the π^0 spectrometer and utilized in the reconstruction of the pion angles. This will provide a cross-check on the behavior of $\text{Re } E_{0+}$, especially above π^+ threshold. As we shall see, the present results support the general behavior depicted in [1].

Let us emphasize that what is presented here are not new experimental data *per se*, but rather is a refined analysis of the angular distributions described in [1]. Previously, the pion angular distributions were reflected in the patterns made by the two π^0 -decay photons as they intercepted various segments of the spectrometer, which we denoted as the “belt-hit” patterns. The “belts” consisted of five segments, like square doughnuts arranged side by side coaxially. Each belt consisted of a number of lead-glass detectors which, in effect, functioned as a single unit and calorimetry (i.e., the photon energies) was not an issue; nor was it utilized directly. We refer the reader to Ref. [5] for technical details.

Since our earlier communication we have greatly refined our understanding of the calorimetry of the spectrometer and now incorporate the decay photon energies in the reconstruction of the pion angular distributions. For this purpose the “belts” are now resolved into their individual detector components. Note that this has no influence whatsoever on our previous determination of the total cross section. We are simply augmenting the angular distribution information with a more refined resolution.

A joint analysis of the total cross section and the refined angular distributions will be shown to substantiate most of the claims made in [1], with one notable exception. The exception is the P -wave combination we called P (now called P_1 by the community). The present result is about 10% larger than we previously claimed and is in very good agreement with the findings of the recent Mainz measurement [6].

II. NOTATION

At low energy the $^1\text{H}(\gamma, \pi^0)$ cross section is determined by the complex S -wave multipole amplitude E_{0+} and three P -wave amplitudes M_{1+} , M_{1-} , and E_{1+} , which are essentially real quantities in the energy domain of interest. Some economy in formalism obtains by working with linear combinations of the P -wave amplitudes defined as follows [4]:

$$\begin{aligned}
P_1 &= 3E_{1+} + M_{1+} - M_{1-}, \\
P_2 &= 3E_{1+} - M_{1+} + M_{1-}, \\
P_3 &= 2M_{1+} + M_{1-}.
\end{aligned} \tag{1}$$

Let us now define the quantity F_0 by the relation

$$2F_0^2 = \frac{1}{3}(P_1^2 + P_2^2 + P_3^2) \tag{2}$$

or, in terms of the P -wave multipole amplitudes,

$$2F_0^2 = 2M_{1+}^2 + M_{1-}^2 + 6E_{1+}^2. \tag{3}$$

It is a simple matter to show that the total cross section σ may be expressed as

$$\frac{k}{q} \sigma = 4\pi(|E_{0+}|^2 + 2F_0^2), \tag{4}$$

where k and q are, respectively, the incident photon and pion momenta in the c.m. frame. In other words, the total cross section is determined by two quantities, and so once F_0 is known, we may deduce $|E_{0+}|^2$ from the experimental cross section. This is the essence of the procedure employed in [1]. Of course, it is critical to know the energy dependence of F_0 , and we will return to this point later, since it has emerged as a point of contention in the literature.

We now turn to the differential cross section in the πN c.m. frame. For historical reasons this is usually written as

$$\frac{k}{q} \frac{d\sigma}{d\Omega} = A + B \cos\theta + C \cos^2\theta, \tag{5}$$

where θ is the pion polar angle in the c.m. frame, and A , B , and C are combinations of the S - and P -wave multipole amplitudes. At this point we digress from the conventional notation and rewrite the differential cross section as

$$\frac{k}{q} \frac{d\sigma}{d\Omega} = a + b(1 - \cos\theta) + c \sin^2\theta. \tag{6}$$

Our preference for this form is purely technical. Under all the theoretical scenarios we have examined, the coefficients a , b , and c are positive definite [unlike those in Eq. (5)], and so the differential cross section Eq. (6) may be envisaged as the superposition of three prototype ‘‘cross sections’’ weighted by the coefficients a , b , and c . This interpretation is basic to our Monte Carlo simulations of the observed angular distributions, and further details are described in Appendix A. The coefficients in Eq. (6) are given in terms of E_{0+} , P_1 , and F_0 as follows:

$$\begin{aligned}
a &= (\text{Im } E_{0+})^2 + (\text{Re } E_{0+} + P_1)^2, \\
b &= -2P_1 \text{Re } E_{0+}, \\
c &= 3F_0^2 - \frac{3}{2}P_1^2.
\end{aligned} \tag{7}$$

We have chosen F_0 as an independent variable since it occurs naturally in the total cross section, Eq. (4), as the *sole* P -wave representation. The quantity P_1 is identical to the

quantity P employed in [1]. Note that the above coefficients are a function of two P -wave amplitudes (F_0 and P_1) and two S -wave amplitudes, and so the system is underdetermined given a , b , and c . In the analysis we will therefore employ a model for $\text{Im } E_{0+}$ (as we did in [1]) and later demonstrate the general insensitivity to the model. The fit to the angular distributions will thus ultimately be governed by the three quantities $\text{Re } E_{0+}$, P_1 , and F_0 .

Let us now address the question of the energy dependence of the P -wave multipole amplitudes M_{1+} , M_{1-} , and E_{1+} and, therefore, by inference the energy dependence of P_1 and F_0 . This is the point of contention mentioned earlier. For several years it was assumed that near threshold the P -wave multipoles were proportional to the simple product kq , which can be traced to a brief line in the book by Amaldi *et al.* [7]: ‘‘from elementary analyticity requirements.’’ More recently, however, Bernard *et al.* [4] have argued that this is incorrect and that near threshold the amplitudes are proportional to q , not kq . Certainly to lowest order there is no debate, since k may be expressed as a power series in q^2 . Our concern from the *practical* point of view is the prescription which best describes the physical amplitudes over an energy range of, say, 25 MeV.

In [1] we concluded that the quantity F_0/kq displays no pronounced energy dependence over 25 MeV, although the situation with respect to P_1/kq was somewhat less clear. In accordance with that tentative conclusion, let us again adopt the Amaldi conjecture and write

$$F_0 = f_0 \cdot kq, \tag{8a}$$

$$P_1 = p_1 \cdot kq, \tag{8b}$$

where the ‘‘reduced’’ amplitudes f_0 and p_1 are supposed to be constants. In these definitions, k and q are expressed in units of the charged pion mass m_π .

Given a suitable model for $\text{Im } E_{0+}$, we therefore have three independent parameters ($\text{Re } E_{0+}$, f_0 , and p_1) to be determined from the angular distributions, together with the additional constraint supplied by the total cross section data.

The model we employ for $\text{Im } E_{0+}$ is a very general one since it derives from the particular constraints of unitarity on the various pion channels available to the γp reaction. More specifically, the imaginary amplitude can be pictured as arising from two-step rescattering processes such as $\gamma p \rightarrow \pi^+ n \rightarrow \pi^0 p$ once the π^+ threshold is crossed. (The $\pi^0 p \rightarrow \pi^0 p$ rescattering contribution is negligible and will be ignored.) While technical details may vary, most authors converge on similar results for $\text{Im } E_{0+}$ [4,8,9]. One obtains

$$\text{Im } E_{0+} = \bar{q} F_{\text{cx}} E_{0+}^B(\pi^+, \bar{q}), \tag{9}$$

where \bar{q} is the on-shell π^+ momentum evaluated at the π^0 production energy, F_{cx} is the S -wave $\pi^+ n \rightarrow \pi^0 p$ charge exchange amplitude, and $E_{0+}^B(\pi^+, \bar{q})$ is the Born amplitude for the $p \gamma \rightarrow \pi^+ n$ channel. In our approximation $\text{Im } E_{0+}$ vanishes below the π^+ threshold.

The charge exchange amplitude is surprisingly constant, more or less, up to rather high energies [10]. Therefore we will employ the familiar low energy expression in terms of the isospin-1/2 and -3/2 scattering lengths,

$$F_{\text{cx}} = \frac{\sqrt{2}}{3} (a_1 - a_3), \quad (10)$$

where [11]

$$a_1 - a_3 = 0.275/m_\pi. \quad (11)$$

Finally, the Born amplitude is calculated as in Ref. [9] with the πNN coupling constant $f^2 = 0.0796$. Note that the energy dependence of $E_{0+}^B(\pi^+, \bar{q})$ is not negligible over the energy domain of the present work, and so we do not simply employ the threshold value in Eq. (9).

Although the model for $\text{Im } E_{0+}$ as given by Eqs. (9)–(11) is rather tightly constrained, it was observed in [9] that an upward renormalization of about 13% was necessary to obtain agreement with the (then existing) information available from various multipole analyses. Those analyses are now somewhat dated, perhaps making the renormalization an open question. On the other hand, Bernard *et al.* [4] achieved a rather nice internal consistency with their own theoretical investigations when they compared with the renormalized $\text{Im } E_{0+}$ of [9]. In using Eq. (9), we will therefore explore both options. Throughout this paper the term “ $\text{Im } E_{0+}$ ” refers to Eqs. (9)–(11), while “renormalized $\text{Im } E_{0+}$ ” means the amplitude renormalized upward by 13%.

III. P-WAVE AMPLITUDES F_0 AND P_1

Our primary objective is to extract $\text{Re } E_{0+}$ from the pion angular distributions (Sec. V). To this end we first begin by examining the energy dependence of the two P -wave amplitudes F_0 and P_1 . In particular, we will demonstrate that the conjecture expressed by Eq. (8a) indeed yields a good description of F_0 up to $E_\gamma = 170$ MeV. This amplitude is the sole P -wave representation in the total cross section [recall Eq. (4)], and the conjecture, tentatively confirmed in [1], was a key factor there in the extraction of the S -wave component.

Analysis of the angular distributions proceeds as outlined in Appendix A. The amplitudes F_0 and P_1 are parametrized according to Eq. (8), but no continuity as a function of energy is enforced at this preliminary stage. That is, the reduced amplitudes f_0 and p_1 are treated as free parameters at each energy, as is $\text{Re } E_{0+}$, while $\text{Im } E_{0+}$ is given by the model in the previous section.

In the original measurements, each angular distribution subtended an energy domain of about 0.5 MeV as determined by the resolution of the individual detector channels of the photon-tagging apparatus. The results for $\text{Re } E_{0+}$ presented in [1] derive from combinations of adjacent pairs of channels. Here we will work with groupings of four channels, and so each angular distribution subtends about 2 MeV.

The reduced amplitudes f_0 from these energy-independent analyses are shown in Fig. 1. Within the indicated errors, f_0 is constant as a function of energy and therefore the ansatz, Eq. (8a), suffices for a *practical* description of F_0 . Without the extra factor of k , the results would display a marked upward slope that is definitely incompatible with the ansatz $F_0/q = \text{const}$.

Let us briefly consider the model dependence as embodied in $\text{Im } E_{0+}$ by repeating the analysis of f_0 , but using the renormalized version of $\text{Im } E_{0+}$. With respect to Fig. 1 the

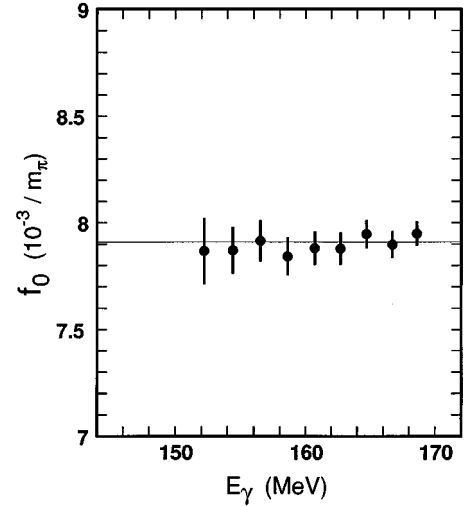


FIG. 1. Reduced amplitude $f_0 = F_0/kq$ as a function of energy. These results are derived from energy-independent analyses, where f_0 and p_1 are free at each energy. The line corresponds to the weighted mean value $\bar{f}_0 = 7.91$.

resulting changes are minimal—for example, the higher energy points are reduced by roughly one standard deviation. More quantitatively, the weighted mean value of the f_0 portrayed in Fig. 1 is

$$\bar{f}_0 = 7.91 \pm 0.03 \quad (12)$$

in units of $10^{-3}/m_\pi$. With the renormalized amplitude one finds

$$\bar{f}_0 = 7.85 \pm 0.03. \quad (13)$$

Thus a 13% variation in $\text{Im } E_{0+}$ translates into roughly a 1% change in \bar{f}_0 .

To summarize the discussion of F_0 , we have demonstrated that Eq. (8a) is certainly an appropriate parametrization of the amplitude and that the effective value for f_0 is quite insensitive to the theoretical uncertainty surrounding $\text{Im } E_{0+}$. Finally, the effective f_0 as given by Eq. (12) is in excellent agreement with the value $f_0 = 7.90 \pm 0.03$ as deduced in [1]. All the tentative conclusions concerning f_0 in that work have now been substantiated.

We now turn to the remaining P -wave amplitude, P_1 as defined in Eq. (1) and as parametrized by Eq. (8b). The fitting of the angular distributions proceeds as before, except that f_0 is now frozen at the value Eq. (12), independent of energy. The resulting reduced amplitudes p_1 are displayed in Fig. 2. They are nearly identical to the corresponding p_1 from the previous free fit, as is to be expected from Fig. 1.

Concerning the model dependence of the amplitudes in Fig. 2, we find these results to be quite insensitive to the uncertainty in $\text{Im } E_{0+}$ just as was observed for f_0 . *Thus, as far as the P -wave amplitudes are concerned, precise knowledge of $\text{Im } E_{0+}$ is not a significant issue.*

The weighted mean value of the reduced amplitudes displayed in Fig. 2 is

$$\bar{p}_1 = 10.26 \pm 0.10 \quad (14)$$

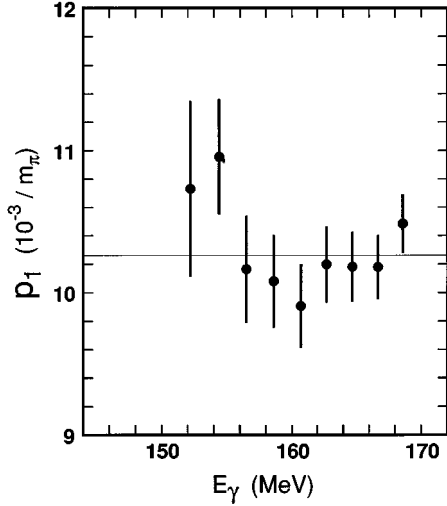


FIG. 2. Reduced amplitude $p_1 = P_1/kq$ as a function of energy. For this analysis f_0 is fixed at the mean value $\bar{f}_0 = 7.91$, independent of energy. The line corresponds to the weighted mean value $\bar{p}_1 = 10.26$.

in the usual units. However, unlike the situation with F_0 , we do not believe that Fig. 2 provides compelling evidence that P_1 is best described by the kq dependence of Eq. (8b). In [1] we also alluded to a mild increase in p_1 with decreasing energy, based on analysis of the “belt-hit” patterns. On the other hand, we can exclude a simple linear dependence of P_1 on q alone and the true behavior probably lies between the kq and q descriptions. However, since we are primarily concerned with $\text{Re } E_{0+}$ above the π^+ threshold, we will pursue the analysis of $\text{Re } E_{0+}$ using the kq dependence of Eq. (8b), where the reduced amplitude p_1 is taken to be independent of energy.

IV. S-WAVE AMPLITUDE $\text{Re } E_{0+}$

All pion angular distributions are now fitted simultaneously. The P -wave amplitudes F_0 and P_1 are parameterized as in Eqs. (8), and the reduced amplitudes f_0 and p_1 are allowed to vary, but are treated as global parameters, independent of energy. Of course, $\text{Re } E_{0+}$ is permitted to vary for each angular distribution. For $\text{Im } E_{0+}$ we employ the unrenormalized model given by Eq. (9) and the following equations. Finally, we extend the analysis closer to the π^0 threshold than before. This was not feasible for the energy-independent analyses of Sec. III since the errors on f_0 and p_1 become understandably excessive near threshold.

The resulting reduced P -wave amplitudes are

$$f_0 = 7.91 \pm 0.03, \quad (15a)$$

$$p_1 = 10.26 \pm 0.10, \quad (15b)$$

which agree with the weighted mean values found previously [Eqs. (12) and (14)]. In comparing with the equivalent parameters presented in [1], excellent agreement exists for f_0 but for p_1 there is about a 10% lower agreement than Eq. (15b). The upward revision in p_1 is mainly a reflection of the improved angular resolution, providing a greater sensitivity to P_1 .

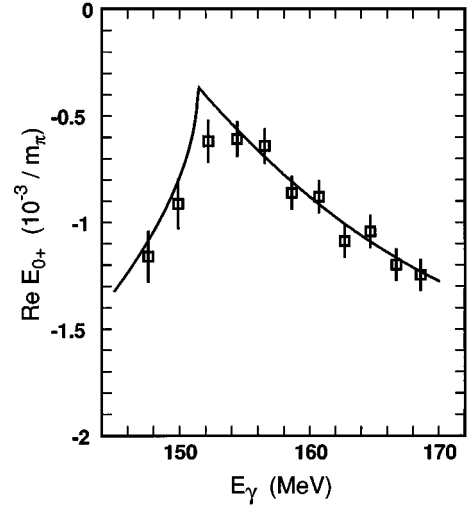


FIG. 3. Multipole $\text{Re } E_{0+}$ as deduced from the pion angular distributions. The associated reduced P -wave amplitudes are given by Eq. (15). The curve is a qualitative description from Ref. [2]. The present results are in general agreement with the earlier values reported in [1].

The corresponding S -wave multipole amplitudes $\text{Re } E_{0+}$ are shown in Fig. 3 and are tabulated in Appendix B. Before commenting on these results, let us consider how they are influenced by the model dependence of $\text{Im } E_{0+}$ by repeating the entire procedure, including variation of the global parameters f_0 and p_1 , using the renormalized version of $\text{Im } E_{0+}$. As expected, $\text{Re } E_{0+}$ is more sensitive than f_0 and p_1 , but not excessively so. None of the resulting $\text{Re } E_{0+}$ shifted by more than 3%, well within the errors we assign to these amplitudes. Unless the actual physical amplitude $\text{Im } E_{0+}$ lies considerably beyond the theoretical uncertainty we have subscribed to it, the results presented in Fig. 3 may be considered essentially model independent. Although we have not pursued this consideration extensively, its origin can be traced to the particular sensitivity of $\text{Re } E_{0+}$ to the angular-asymmetry coefficient b [Eq. (7)], which is independent of $\text{Im } E_{0+}$.

Since we are not convinced that Eq. (8b) is the best practical representation of P_1 , we have repeated the analysis of $\text{Re } E_{0+}$, but now we permit the reduced amplitude p_1 to vary with energy, as in Fig. 2. While some adjustment naturally occurs, the resulting $\text{Re } E_{0+}$ all fall well within the error bars depicted in Fig. 3. Thus, although Eq. (8b) is suspect, it appears to be adequate for our purposes. In a totally free fit, where $\text{Re } E_{0+}$, p_1 and f_0 are permitted to vary with energy, no further change in $\text{Re } E_{0+}$ is observed above 150 MeV (nor in p_1 as noted). Thus the utility of $f_0 = \text{const}$ is only apparent for $\text{Re } E_{0+}$ at the lowest energies.

The amplitudes displayed in Fig. 3 are in satisfactory agreement with our earlier findings [1]. In particular, we definitely confirm the rapid increase in $\text{Re } E_{0+}$ beyond 155 MeV.

The solid curve in Fig. 3 derives from Ref. [2]. That work attempts to give a qualitative description of $\text{Re } E_{0+}$ based on certain phenomenological considerations. There are two free parameters, the threshold value of E_{0+} and the “mass parameter” α , which occurs in the momentum representation of the $\pi^+ n \rightarrow \pi^0 p$ charge exchange amplitude. The threshold

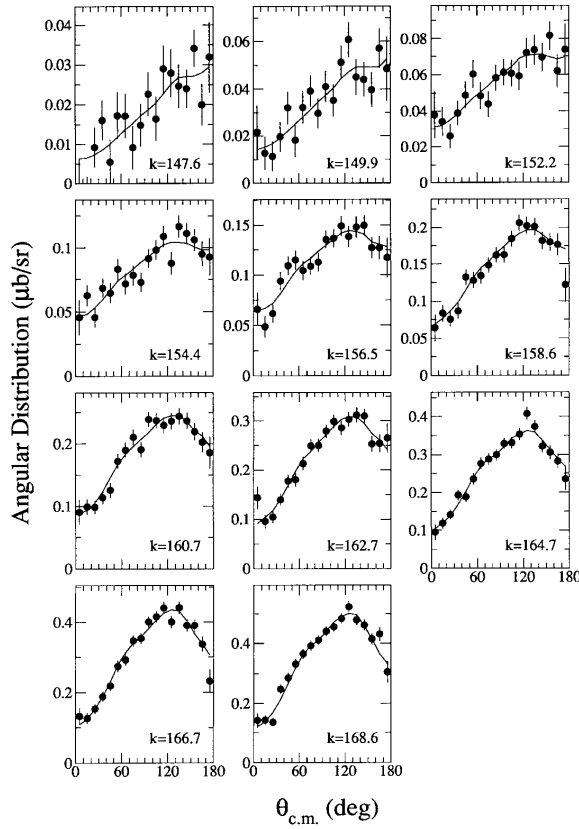


FIG. 4. Pion angular distributions in the πN c.m. system folded with the spectrometer response. Each data point subtends 10° , while each distribution subtends about 2 MeV. Mean photon energies are indicated. The curves represent the simultaneous least-squares fits to all distributions using the “templates” as described in Appendix A. Although the data and fits reflect the angular resolution of the π^0 spectrometer, both are consistent with the total cross section, determined separately. The back-angle drop is largely due to spectrometer distortion.

value is pegged to $E_{0+}(\text{thr}) = -1.32$ as reported from recent experiments [1,6]. The appropriate value for α is not tightly constrained, and as noted in [2], passable descriptions of the experimental charge exchange amplitude [10] obtain for $\alpha = 250\text{--}350$ MeV/c. Although $\alpha = 275$ MeV/c was employed in [2] for purposes of illustration, we find that $\alpha = 250$ MeV/c gives a slightly better description of the present results and is used in Fig. 3.

V. PION ANGULAR DISTRIBUTIONS

The pion angular distributions are illustrated in Fig. 4. The solid curves follow from the simultaneous fitting procedure described above and in Appendix A, and each curve derives from the reduced P -wave amplitudes of Eq. (15), the $\text{Re } E_{0+}$ amplitudes of Fig. 3, and the model for $\text{Im } E_{0+}$ given by Eq. (9). The quality of the fits is reflected in the chi square per degree of freedom: In all cases, we find $\chi^2_{\text{PDF}} \approx 1$.

It must be emphasized that the data and the fitted curves in Fig. 4 do *not* represent the intrinsic photopion differential cross sections. Rather, they represent the true cross sections folded with the angular resolution of the π^0 spectrometer, typically $25^\circ\text{--}35^\circ$ full width at half maximum (FWHM) [5].

The angular response of the spectrometer (not to be confused with absolute π^0 detection efficiency) redistributes pions in angle, but to good approximation conserves their total number. Thus, although slightly distorted, the data and fits of Fig. 4 are still consistent with the total cross section σ as measured separately.

One particular distortion, evident in Fig. 4 at the highest energies, is the slight dent at $\theta = 90^\circ$. While not pronounced, it nevertheless lends further support to our Monte Carlo model of the spectrometer. The relative magnitude of the dent is predicted to decrease with decreasing energy, as demonstrated in [5].

Although not unfolded from the angular response, the results portrayed in Fig. 4 strongly reflect the intrinsic pion angular distributions. One sees, for example, the marked angular asymmetry at low energy, caused by dominance of the b term of Eq. (6) as the P waves recede in strength. At high energy where the P waves are important, a trend towards symmetry starts as the c term in Eq. (6) gathers strength.

Finally, let us compare with the recent differential cross sections from Mainz [6,12]. Where the energies overlap, the differential cross sections appear to be in agreement as far as their angular dependence is concerned. However, a visual inspection suggests that the present results are slightly larger in magnitude. This discrepancy may be traced to the total cross sections, where those in [1] tend to be a bit larger than the total cross section presented in [6].

VI. DISCUSSION

Given F_0 and P_1 , it is possible to make a statement about the other P -wave amplitudes P_2 and P_3 , but only through the combination $P_2^2 + P_3^2$. For the sake of argument, we adopt the kq dependence for all amplitudes, in which case we have the relation between the reduced amplitudes,

$$p_{23}^2 = 3f_0^2 - \frac{1}{2}p_1^2,$$

where, following [6], we define

$$p_{23}^2 = \frac{1}{2}(p_2^2 + p_3^2).$$

Using Eq. (15), one then finds

$$p_{23} = 11.62 \pm 0.08, \quad (16)$$

which compares favorably with the Mainz result $p_{23} = 11.44 \pm 0.09$ [6].

In view of our upward revision of p_1 , let us briefly revisit the estimate given in [1] for the electric quadrupole multipole E_{1+} or, more specifically, the reduced amplitude e_{1+} . From Eq. (1) the reduced amplitudes are related by

$$p_1 = 3e_{1+} + m_{1+} - m_{1-}.$$

Drawing upon various theoretical predictions, we have assembled an estimate for the above magnetic dipole combination, $m_{1+} - m_{1-} = 11.0 \pm 0.4$ (see [1]). This together with the revised p_1 of Eq. (15b) yields a new estimate for e_{1+} ,

$$e_{1+} = -0.25 \pm 0.17, \quad (17)$$

as compared with our earlier result $e_{1+} = -0.60 \pm 0.23$. This downward revision in e_{1+} is certainly in much better accor-

dance with theory. Contemporary theory, including CHPT, typically predicts $e_{1+} \leq -0.2$. Of course a definitive statement about E_{1+} will require polarization degrees of freedom to disentangle the P -wave multipoles, and this is currently under active study at Mainz.

We end with a remark concerning the energy dependence of the amplitude F_0 , defined in terms of the fundamental P -wave multipoles by Eqs. (2) and (3). While it has been argued [4] that these multipoles (and hence F_0) should vary as q in the threshold region, we have found that Eq. (8a) provides a better practical description of F_0 over an extended energy domain. We believe the theoretical treatment of the $\Delta(1232)$ resonance could be the source of the discrepancy, at least judging from a recent study by Pilling and Benmerrouche [13]. Those authors employed an effective Lagrangian as in Ref. [14], where the $\Delta(1232)$ is included as an explicit degree of freedom. The $\Delta(1232)$ is, of course, also incorporated in the CHPT calculations [4], but is subsumed in a contact term. If the resonance contributions are excluded, everyone agrees that F_0 develops in proportion to q . Let us now focus on the Pilling version and consider the quantity F_0/kq . At the Born level, one observes that F_0/kq decreases monotonically with energy due to the increasing k in the denominator. However, the contribution to F_0/kq from the $\Delta(1232)$ alone is observed to *increase* monotonically with energy. The net effect with all contributions is that F_0/kq is nearly constant, decreasing by only about 2% between threshold and 170 MeV. In the CHPT calculations [4], the resonance contributions appear to be isolated in the amplitude P_3 , at least to the order considered in the chiral series. One can only conclude that the associated energy dependence, while valid close to threshold, is not practical over a more extended energy domain.

VII. CONCLUSIONS

Pion angular distributions have been assembled using information on the π^0 -decay photon energies not utilized in our previous Rapid Communication [1]. These new distributions represent an improvement in angular resolution over the previous purely geometric “belt-hit” patterns. It is therefore encouraging that, with one exception, analysis of the refined distributions has reconfirmed our previous conclusions. Most important, we verify that the amplitude $\text{Re } E_{0+}$ increases rather quickly above the π^+ threshold, and this presents a challenge to theoretical interpretation. Although phenomenology provides a description (recall Fig. 3), a more fundamental understanding, say through CHPT, still eludes us.

We have reconfirmed that the P -wave amplitude F_0 , defined by Eqs. (2) and (3), is best described by the “Amaldi conjecture” [7]: in other words, it is proportional to the product kq in our energy domain. This dependence was tentatively identified in [1] from the belt-hit patterns and was an important ingredient in the analysis of $\text{Re } E_{0+}$ reported there. Significantly, the constant of proportionality which we call f_0 is identical in both the new and earlier analyses.

The one exception noted above concerns the particular combination of P -wave multipoles denoted by P_1 [Eq. (1)].

To the extent that the Amaldi conjecture applies to P_1 , we now report a reduced amplitude

$$p_1 = 10.26 \pm 0.10,$$

compared to our previous result $p_1 = 9.2 \pm 0.3$, in the usual units of $10^{-3}/m_\pi$. The revised value agrees nicely with the Mainz value [6], $p_1 = 10.02 \pm 0.15$, and is in perfect agreement with the CHPT prediction [4] $p_1 = 10.3$. However, since we are not convinced the kq dependence is necessarily appropriate to P_1 (or, for that matter, is a pure linear dependence on q), the agreement with CHPT may be fortuitous.

Finally, for completeness we note the excellent agreement between the threshold values of E_{0+} as reported by the SAL [1] and Mainz [6] groups:

$$E_{0+}(\text{thr}) = -1.32 \pm 0.05 \pm 0.06 \quad [1]$$

and

$$E_{0+}(\text{thr}) = -1.31 \pm 0.08 \quad [6].$$

ACKNOWLEDGMENTS

This work was supported in part by the Natural Sciences and Engineering Research Council of Canada.

APPENDIX A: FITTING PROCEDURE

In this appendix we address some of the technical details concerning the extraction of $\text{Re } E_{0+}$ and the reduced amplitudes f_0 and p_1 from the observed pion angular distributions. These angular distributions are distorted by the angular response function of the π^0 spectrometer. We do not attempt to remove the response function from the data to produce the intrinsic angular distributions. Rather, we use the Monte Carlo simulations of the spectrometer response to fit to the observed distributions. Furthermore, we ensure that the fitted distributions correspond closely to the total cross section as measured separately with the spectrometer in the “closed” mode.

The new feature of the present analysis is the incorporation of calorimetry information, or measured photon energies, in the reconstruction of the pion angular distributions when the spectrometer is in the “open” mode. The reconstruction algorithm is described in Ref. [5].

As noted in Sec. II, the differential cross section as expressed by Eq. (6) can be viewed conceptually as the superposition of three angular distributions (i.e., three prototype cross sections) weighted by the positive coefficients a , b , and c . Because of the finite pion angular resolution of the spectrometer, each term in Eq. (6) suffers from angular smearing and distortion. The Monte Carlo code is used to produce three “templates” at each energy, corresponding to each of the angular-dependent factors in Eq. (6). Each template reflects how each angular factor is distorted by the spectrometer angular resolution. Superimposing the three templates using appropriate normalization coefficients then

reproduces the observed angular distribution [5].

Although the templates can, in principle, incorporate the absolute pion detection efficiencies of the spectrometer, we use them here only to provide the relative angular response and instead rely on the measured total cross section to provide the absolute overall normalization of the differential measurements. The reason is that the absolute efficiency predicted by the Monte Carlo model is more reliable for the simple closed configuration than for the open geometry of the angular distribution measurements.

Let us consider this overall normalization procedure in more detail. In order not to confuse the absolute coefficients a , b , and c of Eq. (6) with the as-yet unnormalized coefficients, we will denote the latter as α , β , and γ . They are related by

$$[a, b, c] = \eta[\alpha, \beta, \gamma], \quad (\text{A1})$$

where η is the desired normalization coefficient for a given energy. To repeat, the variation in spectrometer response with pion angle is already absorbed in the templates. The observed but unnormalized differential cross section may thus be written

$$\frac{k}{q} \left(\frac{d\sigma}{d\Omega} \right)_{\text{obs}} = \alpha \text{tmp}(1) + \beta \text{tmp}(2) + \gamma \text{tmp}(3), \quad (\text{A2})$$

where $\text{tmp}(i)$ denotes the templates, which themselves are suitably normalized to 4π and $8\pi/3$ when integrated over all angles. These normalizations are appropriate only if the overall detection efficiency of the spectrometer is independent of the pion angular distribution, but this is essentially satisfied since it is only at the highest energies that the Monte Carlo simulations reveal a *relative* efficiency variation approaching a few percent between the three angular functions of Eq. (6). The coefficients in Eq. (A2) are determined by a least-squares fit to the angular distributions. Finally, we utilize the total cross section σ , determined in a separate measurement. It is related to the coefficients a , b , and c of Eq. (6) by

$$\frac{k}{q} \sigma = 4\pi(a + b + \frac{2}{3}c). \quad (\text{A3})$$

From Eqs. (A1) and Eq. (A3) we then obtain

$$\eta = \frac{(k/q)\sigma}{4\pi[\alpha + \beta + \frac{2}{3}\gamma]}. \quad (\text{A4})$$

We find that η increases monotonically with increasing photon energy, in accordance with the predicted decrease in pion detection efficiency from the Monte Carlo simulations [5].

The normalized differential cross section is given by

$$\left(\frac{d\sigma}{d\Omega} \right)_{\text{obs}} = \eta \left(\frac{d\sigma}{d\Omega} \right), \quad (\text{A5})$$

which by construction is consistent with the total cross section σ . Note, however, that the quantity on the left still contains the smearing and distortions caused by the angular resolution of the spectrometer. It is consistent with σ since the angular response redistributes pions, but to a good approximation does not lose them.

TABLE I. Amplitudes $\text{Re } E_{0+}$ as determined in the present work, as a function of the incident photon energy E_γ in the laboratory frame.

E_γ (MeV)	$\text{Re } E_{0+}$
147.6	-1.16 ± 0.12
149.9	-0.91 ± 0.12
152.2	-0.62 ± 0.10
154.4	-0.61 ± 0.08
156.5	-0.64 ± 0.08
158.6	-0.86 ± 0.07
160.7	-0.88 ± 0.07
162.7	-1.09 ± 0.07
164.7	-1.04 ± 0.07
166.7	-1.20 ± 0.07
168.6	-1.25 ± 0.07

The remaining analysis is straightforward. From Eqs. (A1), (A2), and (A5), we have

$$\frac{k}{q} \left(\frac{d\sigma}{d\Omega} \right)_{\text{obs}} = a \text{tmp}(1) + b \text{tmp}(2) + c \text{tmp}(3). \quad (\text{A6})$$

The coefficients here are next rewritten in terms of $\text{Re } E_{0+}$, $\text{Im } E_{0+}$, F_0 and P_1 according to Eq. (7), and F_0 and P_1 in turn are assumed to follow the energy dependence described by Eq. (8). Fixing $\text{Im } E_{0+}$ as described in the main text, a three-parameter fit is made to the now-normalized angular distributions using the templates. This yields $\text{Re } E_{0+}$, f_0 , and p_1 directly.

TABLE II. Amplitudes $\text{Re } E_{0+}$ as determined in Ref. [1].

E_γ (MeV)	$\text{Re } E_{0+}$
145.34	-1.18 ± 0.14
146.50	-1.24 ± 0.09
147.66	-1.11 ± 0.09
148.81	-1.02 ± 0.09
149.94	-0.95 ± 0.09
151.06	-0.85 ± 0.10
152.17	-0.43 ± 0.18
153.28	-0.48 ± 0.14
154.36	-0.36 ± 0.18
155.44	-0.44 ± 0.15
156.51	-0.64 ± 0.12
157.57	-0.53 ± 0.14
158.61	-0.60 ± 0.12
159.65	-0.52 ± 0.15
160.68	-0.82 ± 0.10
161.69	-0.71 ± 0.11
162.69	-0.95 ± 0.09
163.68	-0.96 ± 0.09
164.66	-0.94 ± 0.09
165.63	-1.17 ± 0.08
166.59	-1.10 ± 0.08
167.54	-1.22 ± 0.08
168.47	-1.28 ± 0.08
169.17	-1.44 ± 0.09

APPENDIX B: TABULATED RESULTS

In this appendix we tabulate the results for $\text{Re } E_{0+}$. The values as determined in the present work are summarized in Table I. Each point corresponds to a combination of four detector channels of the photon-tagging system and, as such, subtends about 2 MeV in photon energy.

Since $\text{Re } E_{0+}$ as determined in Ref. [1] have not been previously presented in numerical form, we include them

here in Table II. In that analysis each point combines pairs of detector channels and hence spans about 1 MeV in photon energy.

All values are expressed in units of $10^{-3}/m_\pi$, where m_π is the charged pion mass.

The total cross section and angular distributions are available through electronic mail from the author [15] upon request. The angular distributions are not unfolded from the angular response of the π^0 spectrometer.

-
- [1] J. C. Bergstrom, J. M. Vogt, R. Igarashi, K. J. Keeter, E. L. Hallin, G. A. Retzlaff, D. M. Skopik, and E. C. Booth, *Phys. Rev. C* **53**, R1052 (1996).
 - [2] J. C. Bergstrom, *πN Newsletter* **12**, 1 (1997).
 - [3] J. C. Bergstrom and E. C. Hallin, *Phys. Rev. C* **48**, 1508 (1993).
 - [4] V. Bernard, N. Kaiser, and Ulf-G. Meissner, *Z. Phys. C* **70**, 483 (1996).
 - [5] J. M. Vogt, J. C. Bergstrom, R. Igarashi, and K. J. Keeter, *Nucl. Instrum. Methods Phys. Res. A* **366**, 100 (1995).
 - [6] M. Fuchs *et al.*, *Phys. Lett. B* **368**, 20 (1996).
 - [7] E. Amaldi, S. Fubini, and G. Furlan, *Pion Electroproduction* (Springer-Verlag, Berlin, 1979). See p. 147.
 - [8] A. N. Kamal, *Phys. Rev. Lett.* **63**, 2346 (1989).
 - [9] J. C. Bergstrom, *Phys. Rev. C* **44**, 1768 (1991).
 - [10] G. Höhler, in *Pion-Nucleon Scattering*, edited by H. Schopper, Landolt-Börnstein, New Series, Group 1, Vol. 9b2, Pt. 2 (Springer, Berlin, 1983). See Fig. 2.2.22.
 - [11] R. Koch, *Nucl. Phys. A* **448**, 707 (1986).
 - [12] A. M. Bernstein, E. Shuster, R. Beck, M. Fuchs, B. Krusche, H. Merkel, and H. Ströher, *Phys. Rev. C* **55**, 1509 (1997).
 - [13] T. Pilling and M. Benmerrouche (private communication).
 - [14] M. Benmerrouche, R. M. Davidson, and N. C. Mukhopadhyay, *Phys. Rev. C* **39**, 2339 (1989); R. M. Davidson, N. C. Mukhopadhyay, and R. Wittman, *Phys. Rev. D* **43**, 71 (1991).
 - [15] The total cross sections and angular distributions are available through electronic mail from the author at Bergstro@skatter.usask.ca